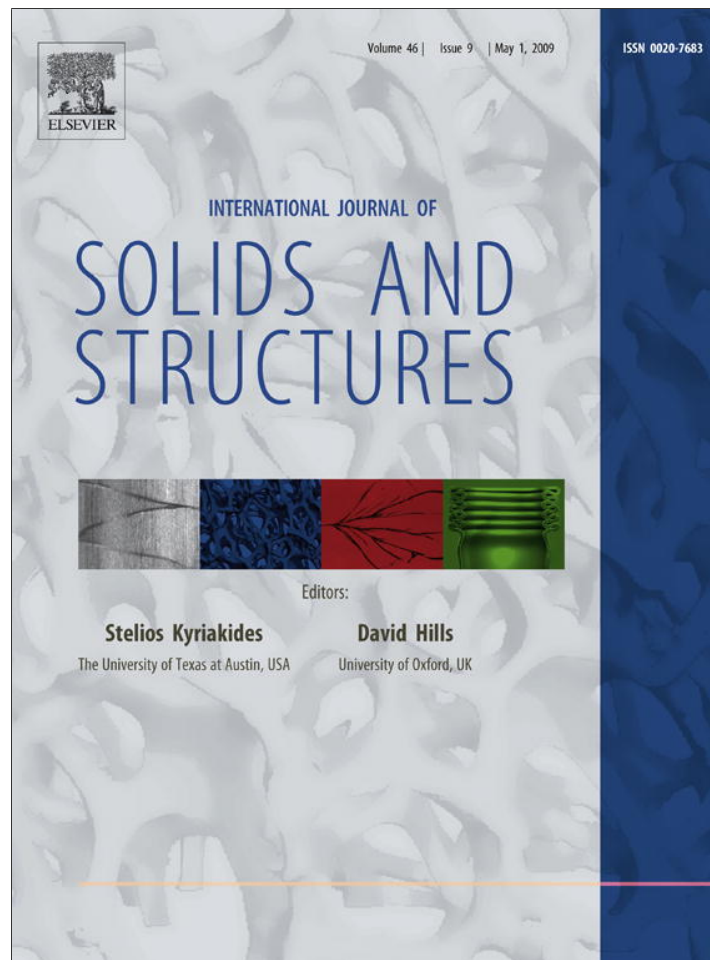


Provided for non-commercial research and education use.  
Not for reproduction, distribution or commercial use.



This article appeared in a journal published by Elsevier. The attached copy is furnished to the author for internal non-commercial research and education use, including for instruction at the authors institution and sharing with colleagues.

Other uses, including reproduction and distribution, or selling or licensing copies, or posting to personal, institutional or third party websites are prohibited.

In most cases authors are permitted to post their version of the article (e.g. in Word or Tex form) to their personal website or institutional repository. Authors requiring further information regarding Elsevier's archiving and manuscript policies are encouraged to visit:

<http://www.elsevier.com/copyright>



Contents lists available at ScienceDirect

## International Journal of Solids and Structures

journal homepage: [www.elsevier.com/locate/ijsolstr](http://www.elsevier.com/locate/ijsolstr)

## Predictive nonlinear constitutive relations in polymers through loss history

David Porter<sup>a,\*</sup>, Peter J. Gould<sup>b</sup><sup>a</sup> Department of Zoology, University of Oxford, South Parks Road, Oxford OX1 3PC, UK<sup>b</sup> QinetiQ Ltd., The Crescent, Bristol Business Park, Coldharbour Lane, Bristol BS16 1EJ, UK

## ARTICLE INFO

## Article history:

Received 30 April 2008

Received in revised form 13 January 2009

Available online 23 January 2009

## Keywords:

Polymer

Equation of State

Constitutive behaviour

High-rate

## ABSTRACT

A model is presented that calculates the highly nonlinear mechanical properties of polymers as a function of temperature, strain and strain rate from their molecular structure. The model is based upon the premise that mechanical properties are a direct consequence of energy stored and energy dissipated during deformation of a material. This premise is transformed into a consistent set of structure–property relations for the equation of state and the engineering constitutive relations in a polymer by quantifying energy storage and loss at the molecular level of interactions between characteristic groups of atoms in a polymer. The constitutive relations are formulated as a set of analytical equations that predict properties directly in terms of a small set of structural parameters that can be calculated directly and independently from the chemical composition and morphology of a polymer.

© 2009 Elsevier Ltd. All rights reserved.

## 1. Introduction

In order to predict the performance of engineering components fabricated from polymers, a reliable combination of equation of state and constitutive model is required as input to simulation tools such as dynamic finite element analysis, FEA. Ideally, the constitutive model should capture the highly nonlinear temperature, strain, and strain rate dependence of mechanical properties such as all the elastic modulus components of the stiffness matrix, and also be able to quantify the elastic and plastic components of the polymer deformation, as well as indicate the most likely mode of failure. The development of high performance materials for demanding engineering applications often runs in a parallel optimisation process, which requires that the engineering property parameters for component design be understood quantitatively in terms of their chemical and morphological structure.

Most models for deformation and yield in a polymer can be traced back to the activated viscosity model of Eyring (1936) and Ree and Eyring (1955), where viscous flow occurs as molecules in a material surmount a potential energy barrier that can be overcome by a combination of thermal and mechanical energy. Earliest tensile models for the yield stress of polymers poly(methyl methacrylate), PMMA, poly(ethyl methacrylate), PEMA, and poly(propylene), PP, from Roetling (1965a,b, 1966) and for PMMA by Bauwens-Crowet and Homes (1964) showed that the Eyring model could be applied to polymers, provided that two different activated processes are used, each with an activation energy with an Arrhe-

nus form. Bauwens-Crowet et al. (1969) updated the model to include poly(carbonate), PC, and poly(vinyl chloride), PVC, to emphasise the two relaxation processes and then to include compression for PMMA (Bauwens-Crowet, 1973), which also featured a simple viscoelastic model with a parallel spring and dashpot combination in series with another spring. Essentially, the models identified yield with the transition from a high elastic modulus glass to a viscous rubberlike state, which is equivalent to the thermally induced glass transition condition. A weakness of these models was an inaccuracy at low yield stresses and higher temperatures close to the glass transition temperature,  $T_g$ , which can be attributed to the use of an Arrhenius activation function for the rate-temperature transformations through  $T_g$ , rather than more elaborate LWF-type functions (Ferry, 1961).

Boyce et al. (1988) considered large strain inelastic deformation using a model based upon molecular structure of a glassy polymer, with restrictions on intermolecular movement controlling the deformation characteristics below yield and  $T_g$ , and entropic resistance dominating the viscoelasticity above yield stress and  $T_g$ . The main features of a stress–strain profile through yield are assigned to different molecular mechanisms, and then parameters are quantified in thermodynamic relations by fitting the model to experimental data. The main practical weakness of such models is the relatively low upper limit of rate of strain at about  $1 \text{ s}^{-1}$ .

Chronologically, two major contributions to understanding mechanical properties in polymers were the evolution of atomistic modelling methods for polymers into a credible predictive tool by Theodorou and Suter (1985, 1986), for example, and the extension of mechanical testing through intermediate ( $10 \text{ s}^{-1}$ ) to high ( $10^4 \text{ s}^{-1}$ ) strain rates by groups such as Walley et al. (1989, 1991) and Walley and Field (1994), for example. Molecular modelling

\* Corresponding author. Tel.: +44 1865 271216.

E-mail addresses: [david.porter@zoo.ox.ac.uk](mailto:david.porter@zoo.ox.ac.uk) (D. Porter), [pjgould@qinetiq.com](mailto:pjgould@qinetiq.com) (P.J. Gould).

(in particular molecular mechanics and dynamics) has become a standard method for calculating the properties of polymers, but the time–temperature scales are not easily applied to real engineering problems and the ‘black box’ character of numerical simulations of large assemblies of atoms is not easily translated into an analytical understanding of dynamic mechanical properties for polymer design and application.

Richeton et al. (2003) reverted to a more continuum treatment of the mechanical properties of amorphous polymers and started by comparing three different models for yield, where the yield and glass transition effects for time temperature superposition used WLF-type relations. Further improvements on these models used a cooperative relaxation effect for segmental relaxation to reproduce new data on a range of polymers to high strain rates, while retaining an essentially thermodynamic approach (Richeton et al., 2005, 2006, 2007).

Mulliken and Boyce (2006) demonstrated that the stress–strain response of PC and PMMA (Mulliken and Boyce, 2006) and PVC (Soong et al., 2006), can be linked back to their dynamic mechanical spectra. In particular, they show that the rate dependence of the  $\alpha$ - and  $\beta$ -transition loss peaks and storage modulus can be used to model the shifts in modulus and yield as a function of temperature and rate. In principle, this again allows the molecular processes responsible for the different transition peaks to be connected (at least qualitatively again) to the features in a constitutive model by invoking molecular level theories for polymer plasticity. In practice, a more conventional empirical and phenomenological approach using springs and dashpots is employed to formulate a strain and rate dependent constitutive model; a pair of parallel springs and dashpots for the  $\alpha$ - and  $\beta$ -processes and an additional nonlinear parallel spring for the limiting elastic behaviour.

Most recently, Zerilli and Armstrong (2007) have formulated a constitutive equation for dynamic deformation behaviour of polymers which advocates the use of a ‘shear activation volume’ to make time–temperature–stress transformations. However, their main modelling refinement is perhaps simply using more parallel spring–dashpot combinations to allow more detailed empirical fitting of experimental data.

While most of the above approaches to modelling dynamic mechanical properties in polymers can be loosely classed as ‘continuum’ or ‘mechanical’, with reference to their ultimate description of mechanical properties in terms of spring–dashpot elements (albeit with a molecular basis), polymer industry has often taken an alternative more chemistry-based approach of using quantitative structure–property relations, QSPR, to relate polymer properties directly to their chemical composition and morphology. Bondi (1968) relates properties to chemical structure through molecular models and provides a strong ‘fundamental’ foundation for later models that tend to make more direct empirical links between structure and properties. For example, the group contribution approach of van Krevelen (1993) is widely used to make rapid estimates of properties simply using group additive parameters. The connectivity indices method of Bicerano (1993), while being an empirical approach, suggests that many polymer properties are linked to structure at a very simple level of nearest-neighbour atomic bonding. Wu (1990, 1992) formulates useful relationships between polymer chain structure (entanglement density and characteristic ratio) and mechanical properties.

Within the QSPR approach, Seitz (1993) demonstrates a very useful series of mainly empirical relationships between molecular structure and mechanical properties, which like Bondi are based largely on molecular concepts. The key point to note here is that Seitz starts from a molecular interaction (potential function) model to calculate the bulk elastic modulus of a polymer as the reference modulus parameter and then uses a relation for Poisson’s ratio to calculate all the other engineering moduli. Yield and strength prop-

erties are essentially empirical fits to molecular structure parameters such as molecular cross-section dimensions, but nevertheless do point to relatively straightforward fundamental relations between molecular structure and dynamic mechanical properties in polymers.

This work attempts to combine the engineering transparency of the continuum approach to constitutive models with the simplicity of QSPR models that make direct relations between mechanical properties and polymer structure, without losing the more fundamental insights into molecular mechanisms provided by molecular modelling. To do this, we use the method of group interaction modelling, GIM, of Porter (1995), which was suggested as a practical modelling tool to predict the thermomechanical properties of polymers in a self-consistent framework that is applicable to any state of matter (crystal, glass, rubber, or liquid) and captures the main features of the highly nonlinear characteristics of polymer viscoelasticity as a function of temperature, strain, and strain rate. This approach allows the role of different structural elements in a polymer to be clearly understood, and thereby leads to a new approach to the design of polymers for the demanding combinations of properties required in modern engineering structures.

## 2. GIM model outline

GIM uses a highly focused molecular level model to calculate the energy stored and dissipated during mechanical deformation. Recent advances in GIM for thermoset resins (Jones, 2005; Foreman et al., 2006) and silk biopolymers (Vollrath and Porter, 2005; Porter and Vollrath, 2008) are then applied here to transform the equation of state and dynamic mechanical profile for a polymer into a nonlinear stress–strain profile that is the basis for the constitutive model. In order to clarify the modelling process, the key steps in the GIM model are:

1. Select the characteristic group of atoms that defines the chemical structure of the polymer, which is usually the mer unit.
2. Assign a limited number of structural parameters to the group that allow its average dimensions and main molecular energy terms to be calculated using either empirical methods or atomistic simulations at whatever appropriate level of complexity and rigour.
3. Use the dimensions and energy terms in a potential function to calculate volumetric properties such as density and thermal expansion.
4. Use the volumetric derivatives of the potential function to calculate pressure and bulk elastic modulus as purely elastic reference parameters that effectively define the limiting high rate (shock) equation of state for the polymer.
5. Calculate the glass transition and crystal melt temperatures as a function of frequency using the elastic instability condition from the potential function with the Born criterion as the point where the second derivative of energy between groups tends to zero.
6. Define and calculate any secondary relaxation points that are usually the onset of skeletal mobility in specific atomic sub-groups.
7. Calculate the total energy dissipation associated with the transitions in the form of the area under the loss tangent curves as a function of temperature, and then assign simple normal distribution functions to quantify the detailed loss tangent distributions with temperature.
8. Combine the reference elastic bulk modulus with the energy dissipation to calculate the engineering properties of bulk and tensile modulus as a function of temperature and fre-

quency; this gives a dynamic mechanical spectrum for the polymer. Essentially, measured modulus values are reduced from their purely elastic value as more energy is converted to heat by molecular redistribution under strain. This includes the transition from glass to rubber as a continuous process.

9. Calculate Poisson's ratio from the combination of bulk and tensile modulus, which allows all the terms in the stiffness matrix to be calculated as a function of temperature and rate.
10. Use temperature as a dummy variable to calculate a combination of strain (thermal expansion) and stress (thermal expansion  $\times$  modulus) to predict a full stress-strain profile through yield, which is determined by the glass transition condition of modulus tending to zero.
11. Calculate post-yield strain softening as stress relaxes back to a low rate limiting yield stress.

### 3. Polymer model

From the summary of the modelling process, radical simplicity of the polymer model is essential for making quantitative predictions of complex mechanical properties tractable. The mean field potential function approach uses ensemble averaged parameter values that can be calculated most simply from chemical structure either empirically using group additivity tables (van Krevelen, 1993; Porter, 1995) or connectivity indices (Bicerano, 1993), or alternatively the parameters can be calculated using atomistic simulations right through to detailed quantum mechanics (Porter and Vollrath, 2008). The main motivation for this form of model is to replace the detailed numerical calculations of molecular dynamics simulations of complex mechanical properties by a series of predictive analytical equations, in which the independently calculated parameters do not have to be obtained by fitting the experimental data they are trying to predict.

For polymers and many organic materials, their response to mechanical deformation is determined largely by the weak van der Waal's forces between groups of atoms normal to the chemically bonded polymer chain axis. Following the lead of molecular mechanics simulations (Theodorou and Suter, 1985) and correlations with pressure-volume observations (Arends, 1993), such forces can be represented by a simple 6-12 Lennard-Jones equation for energy as a function of separation distance between chains. To a good first approximation, the stiffness in the chain axis is large enough for volume,  $V$ , to be proportional to separation distance squared, such that the potential energy well of group interactions,  $E$ , with a depth equivalent to the zero-point cohesive binding energy,  $E_{\text{coh}}$ , at the volume  $V_0$  can be written

$$E = E_{\text{coh}} \left( \left( \frac{V_0}{V} \right)^6 - 2 \left( \frac{V_0}{V} \right)^3 \right) \quad (1)$$

A second expression relates the  $E$  and  $E_{\text{coh}}$  in terms of the positive energy contributions of thermal energy,  $H_T$ , and 'configurational' energy,  $H_c$ , that takes  $E$  out of the well minimum.

$$E = -E_{\text{coh}} + H_c + H_T \quad (2)$$

The term  $H_c$  represents the non-minimum energy of conformers that stabilize the quantum mechanics zero-point vibrational energy of the polymer chains, and can be quantified to a good approximation by values of  $0.04E_{\text{coh}}$  and  $0.106E_{\text{coh}}$  for crystal and amorphous glass states of matter, respectively, which are additive in the fraction of each state. The broader significance of  $H_c$  is discussed in more detail elsewhere (Porter, 1995; Porter and Vollrath, 2008).

The heat capacity of polymers has been investigated extensively by Wunderlich et al. (1989), and the most important contribution to mechanical properties has been shown to be a one-dimensional Debye function of skeletal mode vibrations in terms of number of degrees of freedom per group,  $N$ , the reference temperature of cooperative skeletal vibrations,  $\theta_1$ , and temperature,  $T$ . Other local mode vibrations of atomic groups affect the bulk heat capacity, but do not contribute to the temperature dependence of mechanical properties. GIM simplifies the Debye function into an empirical relation for specific heat capacity,  $C$ , and for ease of calculation has formulated a table of atomic group contributions and selection rules for  $N$  and  $\theta_1$ . If  $R$  is the molar gas constant

$$C \approx NR \frac{\left( \frac{6.7T}{\theta_1} \right)^2}{1 + \left( \frac{6.7T}{\theta_1} \right)^2} \quad (3)$$

Using  $C$  to calculate the thermal energy term,  $H_T$ , in the potential function is necessary, since  $N$  changes with temperature as new degrees of freedom are activated above a number of transition temperatures that play an important role in predicting mechanical properties.  $H_T$  is then given by

$$H_T = \int_0^T C dT \text{ J/mol} \quad (4)$$

Group contribution tables are available for the model parameters of  $E_{\text{coh}}$ , van der Waal's volume,  $V_w$  (where  $V_0 = 1.26V_w$ ), and molecular weight,  $M$ , which allows the model relations to be quantified for any polymer composition and structure (van Krevelen, 1993; Porter, 1995). The zero-point potential function of Eq. (1) can be applied to the local potential well at any temperature simply by using the new equilibrium well depth,  $E_T$ , and volume  $V_T$ .

Equilibrium volumetric properties such as density and volumetric expansion coefficients,  $\alpha$ , are calculated by solving Eqs. (1)–(3) as a quadratic equation in  $(V/V_0)^3$  as a function of temperature. Again due to changes in degrees of freedom at transition temperatures, it is best to calculate volumetric properties using thermal expansion relative to a reference point using an expression for  $\alpha$  in terms of the skeletal heat capacity,  $C$  (Porter, 1995)

$$\alpha \approx \frac{1.38 C}{E_{\text{coh}} R} \quad (5)$$

The utility of this approach for understanding the role of structural elements in a polymer structure is perhaps best illustrated by the change in the parameter  $N$  for degrees of freedom due to crosslinking or branching in a thermoset resin (Jones, 2005; Foreman et al., 2006). Here, the value of  $N$  is reduced by 3 for every chain branch site in the structural group to reflect the loss of vibration freedom due to the normal constraints of the bonding. Thus, properties such as glass transition temperature and thermal expansion coefficient (and thereby mechanical properties) can be predicted as a function of crosslinking or degree of cure. Thus, a clear link between polymer structure and properties makes this a very powerful tool in polymer design or optimisation of a balance of properties.

Table 1 gives a list of the GIM parameter values for the two example thermoplastic polymers of PC, and atactic PMMA. The main problem for quantifying parameters comes in assigning degrees of freedom,  $N$ , for conventional atactic PMMA, which is a mixture of iso- and syndiotactic conformers, each with very different glass transition temperatures that correspond to values of  $N$  of 6 and 9, respectively, due to the mobility constraints imposed by the acrylate side groups. We have adopted a conventional view of a predominance of the syndiotactic form with a fraction of about 0.75 for an average value of  $N = 6.7$  (McRum et al., 1967), which corresponds to a model glass transition temperature of 410 K at a reference frequency of 1 Hz.

**Table 1**  
Model structural parameters and reference properties for the example polymers PC and PMMA: see text.

Parameter/property	PC	PMMA
van der Waal's volume $V_w$ (cc/mol)	139	57
Molecular weight $M$ (D)	254	100
Length in chain $L$ (Å)	11	3.1
Cohesive energy $E_{coh}$ (J/mol)	83,000	45,000
Theta temperature $\theta_1$ (K)	550	290
Activation energy $\Delta H_\beta$ (J/mol)	44,000	70,000
Degrees of freedom:		
$N$	14	6.7
$N_c$	32	6.7
$\Delta N_\beta$	6	2
Dissipation parameter $A$ (GPa <sup>-1</sup> )	1.18	1.60
Cumulative loss:		
$\tan \Delta_\beta$	4.7	8.3
$\tan \Delta_g$	22	57
$T_\beta$ (K) at 1 s <sup>-1</sup>	187 (193)	285 (288)
$T_{gr}$ (K) at 1 s <sup>-1</sup>	427 (423)	410 (378/399)
Density (kg m <sup>-3</sup> ) at 300 K	1230 (1200)	1176 (1170)
Thermal expansion coefficient (10 <sup>-4</sup> K <sup>-1</sup> )	2.18 (2.00)	1.96 (1.96)

Fig. 1 shows predictions of density and thermal expansion coefficient for the two polymers as a function of temperature, using transition temperatures at the reference rate of 1 s<sup>-1</sup>. The predicted values of transition temperatures, density and thermal expansion coefficient at 300 K are given in Table 1, alongside the observed values (given in brackets) (Richeton et al., 2006; Mulliken and Boyce, 2006; van Krevelen, 1993), with which they are in good agreement.

#### 4. Equation of state

Pressure is calculated as a function of volume using the differential of the potential function of Eq. (1)

$$P = \frac{dE}{dV} = \frac{6E_T}{V_T} \left( \left( \frac{V_T}{V} \right)^4 - \left( \frac{V_T}{V} \right)^7 \right) \quad (6)$$

The pure elastic form of bulk modulus,  $B_e$ , is similarly calculated as a derivative of energy or pressure.

$$B_e = V \frac{d^2E}{dV^2} \approx \frac{6E_T}{V_T} \left( 5 \left( \frac{V_T}{V} \right)^4 - 8 \left( \frac{V_T}{V} \right)^7 \right) \quad (7)$$

which simplifies at low strains to

$$B_e \approx 18 \frac{E_T}{V_T} \quad (8)$$

Without considering the specific case of highly oriented polymeric fibres, many polymers at the continuum level behave as isotropic materials with a random distribution of molecular chain orientations or crystal domains. This allows us to use the pure elastic form of bulk modulus as the reference elastic parameter from which other elastic modulus terms can be derived in the following sections. However, it is interesting here to illustrate the use of the model for predicting the equation of state for the example polymers PC and PMMA under high pressure shock conditions (a reference volumetric elastic state, where the deformation time scales are too short to allow relaxation processes due to molecular redistribution) to demonstrate the broad applicability of the model and its practical utility relative to molecular dynamics simulations (Porter and Gould, 2003, 2006). This condition also dominates many impact events that are important for engineering.

At very high pressures associated with shock Hugoniot states, we also need to take account of the smaller volumetric strain due to the shrinkage in the relatively stiff chain axis, which has a modulus of the order  $Y_p \approx 240$  GPa in a simple poly(ethylene) structure, for example. As a good first approximation, we find that the shrinkage in the two axes can be added without accounting for synergy in the thermal energy function due to associated changes in  $\theta_1$  as a pressure dependent heat capacity. The chain axis modulus is suggested to have a volume dependence due to reduced normal cross-sectional area, which simultaneously increases modulus and reduces force at a given pressure.

$$Y_p \rightarrow Y_p \left( \frac{V_0}{V} \right)^2 \quad (9)$$

For most hydrocarbon polymers, the stiffness in the chain axis due to bending of chemical bonds is approximately constant if the *trans*- and *gauch*-states are taken into consideration, such that  $Y_p$  is inversely proportional to chain cross-sectional area. An anomaly due to chain axis deformation has been noted previously, where phenyl rings collapse at a compressive stress of about 20 GPa to give a step-wise reduction in volume and shifts in the Hugoniot  $U_s-U_p$  plots seen in the PC example in Fig. 2 (Porter and Gould, 2003). Particle and shock velocities,  $U_p$  and  $U_s$ , respectively, are calculated by the

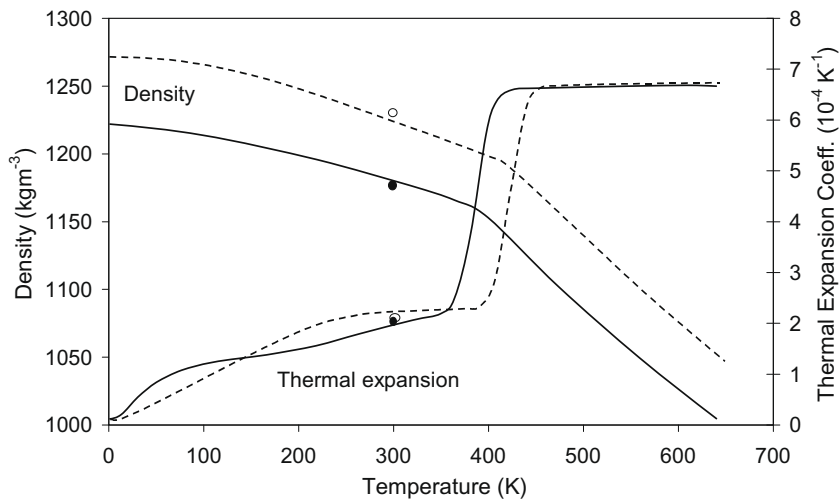


**Fig. 1.** Predictions of density and thermal expansion coefficient for the PC (dashed lines) and PMMA (solid lines) examples, with observed values shown as points for reference (van Krevelen, 1993).

usual expressions in terms of model parameters that can all be predicted by the model (Porter and Gould, 2006).

$$U_p = \sqrt{\frac{P(1 - V/V_T)}{\rho_T}}; \quad U_s = \sqrt{\frac{P}{(1 - V/V_T)\rho_T}} \quad (10)$$

Fig. 2 shows a predicted pressure–volume line for PC against experimental data points obtained from impact experiments (Carter and Marsh, 1997). Volume is in the form of  $V/V_T$ , and the parameters required for Eq. (6) are calculated as  $V_T = 207$  cc/mol and  $E_T = 55.3$  kJ/mol. The deviation between model and observation above about 20 GPa is proposed to be due to the collapse of phenyl rings to a more compact, but energetically unfavourable, form (Porter and Gould, 2003).

Fig. 3 shows the common form of a  $U_s-U_p$  plot for PMMA from plate impact experiments in the form of a line predicted by Eqs. (6) and (10) against experimental data points (Carter and Marsh, 1997). Here the calculated model parameters are  $V_T = 84.7$  cc/mol and  $E_T = 29.2$  kJ/mol and  $\rho_T = 1180$  kg m<sup>-3</sup>.

The role of the bulk modulus parameter  $B_e$  is that of a reference pure elastic modulus term, from which all the other engineering modulus parameters in the full stiffness matrix can be calculated. To do this, in the next section we discuss the role of energy dissipation under non-ideal generalised deformation geometries and at finite rates, where molecular redistribution occurs to minimise the local potential energy of intermolecular interactions.

### 5. Energy dissipation and loss tangent

With bulk modulus as the reference parameter for elastic energy storage, we now need to derive relations for energy dissipation at the molecular level to quantify the full viscoelastic response of a polymer. Since energy dissipation processes in a polymer are still not fully explained or predicted quantitatively at a fundamental level, we need to quantify loss processes in a pragmatic way that is practically useful. We believe that establishing the most important characteristics of loss processes in this way will then act as a guide how to make predictions directly from atomic level simulations.

Loss processes are split into two forms. The first is called thermomechanical loss, where mechanical energy is transformed irreversibly into heat simply by means of changes in thermal parameters that are induced by mechanical loading. The second is the energy dissipated through transition events, where the number of active degrees of freedom changes in a polymer due to changes in temperature or mechanical loading. Generally, the mechanical loss spectrum of a polymer consists of a low-level baseline due to thermomechanical loss and large peaks due to transition events, which are considered separately below.

The parameter used to quantify energy dissipation is loss tangent, which is defined quite loosely here as the ratio of energy dissipated to energy stored in a deformation cycle at a given temperature and rate or frequency.

#### 5.1. Thermomechanical loss

As mechanical load is applied to a material, the distances between atoms and molecules change. This, in turn, changes the elastic modulus of the polymer, which then changes thermal parameters such as the reference temperatures in the Debye models for heat capacity. This process effectively converts mechanical energy irreversibly to heat, and was used in the first formulation of GIM to quantify loss tangent as being proportional to the temperature gradient of bulk elastic modulus (Porter, 1995). The proportionality constant,  $A$ , is determined by structural parameters of the characteristic mer unit, and takes a range of values for most polymers in the range 1–2 GPa<sup>-1</sup>.

$$\tan \delta = -A \frac{dB}{dT} = -\frac{1.5 \times 10^5 L}{\theta_1 M} \frac{dB}{dT} \quad (11)$$

where  $L$  is the length of the mer unit in the polymer chain axis and  $M$  is its molecular weight. Since the changes in bulk modulus with temperature can be calculated in using Eq. (8), the baseline thermomechanical loss tangent can be calculated quite simply using the model parameters that characterise the molecular structure, and takes a value of the order 0.01.

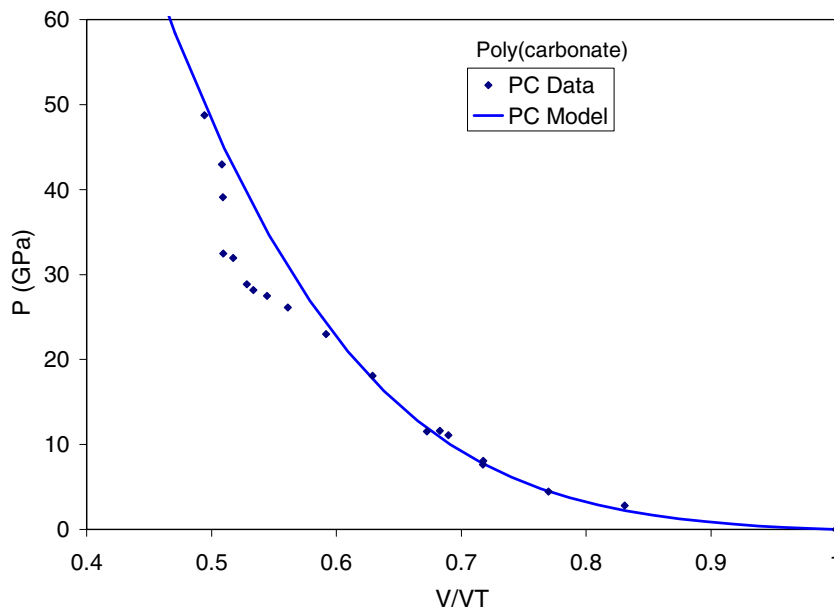


Fig. 2. Comparison of predicted and experimental (Carter and Marsh, 1997) compaction of PC under shock conditions.

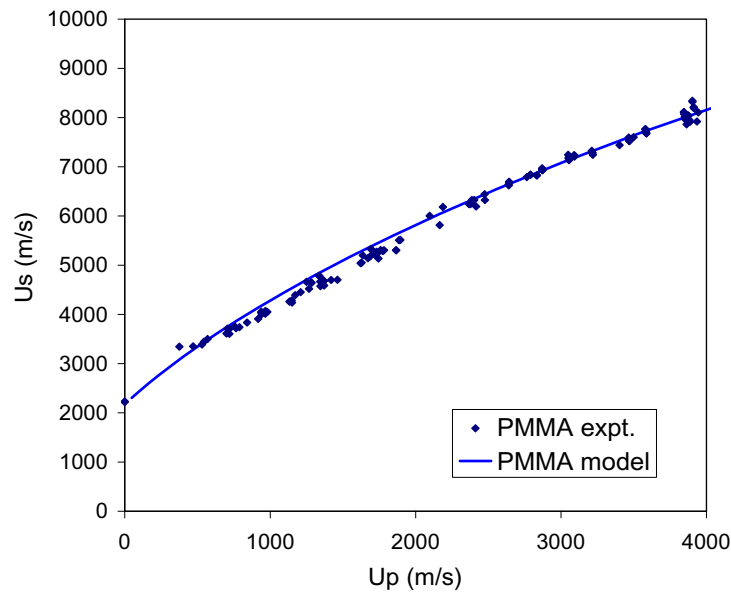


Fig. 3. Comparison of predicted and experimental (Carter and Marsh, 1997) shock Hugoniot relations for PMMA.

### 5.2. Loss peaks due to transition events

In this model, peaks in loss tangent are attributed to transition events in a polymer, where the number of degrees of freedom in the mer unit changes through a limited range of temperatures. Again rather simplistically, we split these events into two types. The upper temperature peak is associated with the glass transition at  $T_g$ , and is due to the development of intermolecular motion above this temperature. Lower temperature peaks are here attributed to the development of degrees of freedom due to the activation of intramolecular skeletal modes of vibration that are constrained at lower temperatures around a reference temperature  $T_\beta$ , using the usual nomenclature for polymer relaxations (McRum et al., 1967).

A considerable body of experimental data is available for dynamic mechanical loss peaks in polymers, which has allowed models to quantify their position, magnitude, and distribution to be developed as a function of temperature and rate (McRum et al., 1967). Of these three descriptors, distribution is still the most difficult to quantify. We start here by looking at the glass transition, since previous models have been successful in predicting polymer properties in a wide range of polymer types and applications.

#### 5.2.1. Glass transition

The most important temperature for a polymer is its glass transition temperature  $T_g$ , which can be calculated using a relation derived from the potential functions by calculating the temperature of the Born elastic instability criterion, where the elastic modulus tends to zero with the second differential of energy with respect to separation distance (Born, 1939; Porter and Vollrath, 2008). The increased mobility of the atomic groups in the polymer chain increases the number of degrees of freedom to  $1.5N$ , where two normal modes gain an extra translational degree of freedom in each chain atom, for example. A reference value of  $T_{gr}$  at a measuring rate of 1 rad/s can be predicted by GIM relations in the model structural parameters (Porter, 1995)

$$T_{gr} = 0.224\theta_1 + 0.0513 \frac{E_{coh}}{N} \quad (12)$$

At a physical level, this relation says simply that  $T_g$  increases with increasing chain stiffness and intermolecular binding energy, and  $T_g$  decreases with increasing degrees of freedom.

$T_g$  changes with frequency or rate and a number of methods are available to calculate this dependency, such as the LWF approach (Ferry, 1961). A typical change of  $T_g$  is about  $4^\circ$  per decade of rate change. GIM uses a relation similar in form to the Vogel–Fulcher function, which has the advantage that all the parameters can be quantified in terms of model structural parameters, such that  $T_g$  at the frequency,  $f$ , is calculated using

$$f = f_0 \exp\left(-\frac{1280 + 50 \ln \theta_1}{T - T_{gr} + 50}\right) \quad (13)$$

where  $f_0$  is the frequency of skeletal mode vibrations, and is calculated from the reference temperature  $\theta_1$  using the relation in Boltzmann's constant,  $k$ , and Planck's constant  $h$

$$f_0 = \frac{k\theta_1}{h} \quad (14)$$

The most important attribute of the glass transition is that the tensile and shear elastic moduli of a polymer reduce by a factor of about 1000 above  $T_g$ . In this model, we identify the thermal glass transition condition directly with the mechanical yield point of a polymer, where modulus tends to zero. Consequently, the frequency dependence of  $T_g$  becomes the rate dependence of the yield point: note here that we adopt the broad simplification that strain rate is numerically equivalent to the angular frequency,  $2\pi f$ , rather than make detailed calculations for any specific deformation geometry (Mulliken and Boyce, 2006).

In addition to the position of the elastic instability point at  $T_g$  or the yield point, we now need to calculate the magnitude of energy dissipation through this point. To do this, the cumulative loss tangent through the  $T_g$  loss peak,  $\tan \Delta_g$ , is defined as the total area under the loss tangent peak, without including the baseline thermomechanical loss. A predictive expression for this loss parameter has been derived in previous work by quantifying the energy changes in the polymer due to the onset of new translational degrees of freedom at  $T_g$  (energy dissipated) relative to the energy required to take the polymer through the transition (energy stored) (Porter, 1995)

$$\tan \Delta_g \approx 0.0085 \frac{E_{\text{coh}}}{N_c} \quad (15)$$

where  $N_c$  is the number of active degrees of freedom in the chain axis that can absorb energy when stretched, and can be calculated using group contribution tables in the usual way. For the example polymers, PC has  $E_{\text{coh}} = 83$  kJ/mol and  $N_c = 32$  for  $\tan \Delta_g = 22$ , and atactic PMMA has averaged values of  $E_{\text{coh}} = 45$  kJ/mol and  $N_c = 6.7$  for  $\tan \Delta_g = 57$ .

The distribution of  $\tan \delta$  as a function of temperature through  $T_g$  is approximated by assuming a simple Gaussian distribution around the peak position. For a polymer composed of single mer unit types, the distribution of parameter values due to many different intermolecular interactions tends to a limiting low value of standard deviation in temperature of  $s_g \approx 6^\circ$  at a reference rate of  $1 \text{ s}^{-1}$  due to the inherent natural distribution of kinetic energy in the atomic groups. The model distribution function takes the form

$$\tan \delta_g = \frac{\tan \Delta_g}{s_g \sqrt{2\pi}} \exp\left(-\frac{(T - T_g)^2}{2s_g^2}\right) \quad (16)$$

In this work, we assume that the thermal glass transition condition is physically equivalent to mechanical yield at the elastic instability point where modulus tends to zero under a combination of thermal and mechanical conditions in the potential function. We will show that this general equivalence makes the need for arbitrary activation criteria for yield, such as an activation volume, redundant (Zerilli and Armstrong, 2007)

### 5.2.2. Beta peaks

While the mechanism, position, distribution, magnitude, and rate dependence of glass transition events can be explained and quantified by a number of different models or experimental techniques, the same cannot be said about low temperature relaxation processes that give mechanical loss peaks often well below the glass transition.

In GIM, the origin of beta loss peaks is the activation of intramolecular degrees of freedom as constraints on specific groups of atoms are relaxed through and above  $T_\beta$ . For many engineering polymers such as PC, this is attributed to the onset of torsional motion in main-chain aromatic rings. For branched polymers such as PMMA, it is the relaxation of stronger polar bonds between side chains (Mulliken and Boyce, 2006). These relaxation events can be treated as a first order Arrhenius function in activation energy and the frequency of skeletal mode vibrations in the polymer chain,  $f$ . The activation energy,  $\Delta H_\beta$ , for such events can be calculated using quantum mechanics simulations of the energy to exceed the rotational barriers that constrain the groups of atoms. For aromatic rings, this energy is about 40–50 kJ/mol that depends upon the adjacent chain atoms (Bicerano and Clark, 1992; Hutnik et al., 1991), and for PMMA the relaxation of the ester side groups is taken to be about 70 kJ/mol in this work to fit experimental data using the relation (Mulliken and Boyce, 2006; McRum et al., 1967)

$$T_\beta = \frac{-\Delta H_\beta}{R \ln\left(\frac{r}{2\pi f_0}\right)} \quad (17)$$

where  $R$  is the gas constant and  $r$  is the applied rate of strain relative to the angular frequency of skeletal mode vibrations  $2\pi f_0$  from Eq. (14). A typical change of  $T_\beta$  is about  $15^\circ$  per decade of rate change.

The magnitude of the beta loss peaks is again quantified by a cumulative loss tangent,  $\tan \Delta_\beta$ . Predictive equations for  $\tan \Delta_\beta$  are far less defined than for the glass transition, but the same general approach is adopted here of taking the ratio of energy change through the transition due to the onset of  $\Delta N_\beta$  skeletal degrees of freedom through a temperature interval of  $\Delta T_\beta$  with  $N_c$  degrees of freedom in the chain at  $T_\beta$  to suggest

$$\tan \Delta_\beta \approx \frac{T_\beta}{\Delta T_\beta} \frac{\Delta N_\beta}{N_c} \approx 25 \frac{\Delta N_\beta}{N_c} \quad (18)$$

The general proportionality between  $T_\beta$  and  $\Delta T_\beta$  was demonstrated in the original GIM model for beta relaxations, but the quantitative value of 25 for the proportionality constant has been found by extensive modelling and correlations between the width of the intrinsic beta relaxation peak at half height and  $T_\beta$ . This proportionality tells us that the peak distribution width must increase as the peak temperature increases with increasing rate or frequency to maintain constant total cumulative loss tangent area under the peak.

The distribution of beta peaks is much broader than for the glass transition, due to the large number of different intramolecular conformations that an amorphous polymer chain can adopt to influence  $T_\beta$ . In principle, detailed molecular dynamics simulations of molecular motion should be able to predict the distribution width  $\Delta T_\beta$  (Hutnik et al., 1991). However, we have not yet found a satisfactory method that gives good correlation with observation. In practice, the overall total distribution is usually much broader than for  $T_g$  and can be fitted with a Gaussian distribution to experimental data from a DMA analysis, often giving a standard deviation,  $s_\beta$ , in the range 40–80°, with a typical value of 60° at a rate of  $1 \text{ s}^{-1}$  that is used generally in this work.

## 6. Engineering moduli

The previous sections have outlined how storage and dissipation of mechanical energy of deformation in a polymer can be described quantitatively by the two reference parameters of elastic bulk modulus,  $B_e$ , and loss tangent, respectively. Most important is that these parameters are calculated from the molecular structure and molecular level processes in the polymer and are both temperature and rate dependent. The practically important engineering properties such as Young's modulus, shear modulus, and Poisson's ratio now need to be formulated in terms of these reference parameters.

The first modulus to be considered is the bulk modulus,  $B$ , at lower rates of deformation than the ideal elastic value of  $B_e$  under shock conditions.  $B$  reduces relative to  $B_e$  due to the mechanical energy dissipated as atoms and molecules are rearranged to attain a lower total energy as volume is changed during deformation. The main changes in  $B$  are attributed to the change in the cohesive energy through transitions, where the number of degrees of freedom changes. Previous work has shown that the fractional change in cohesive energy through the glass transition is about 0.5, which is numerically identical to the fractional change in the degrees of freedom that develop through  $T_g$  due to the increased chain mobility,  $\Delta N_g/N$ . For beta transitions, a similar argument is proposed that the fractional change in degrees of freedom,  $\Delta N_\beta$ , relative to the intramolecular skeletal modes,  $N_c$ , gives an equivalent fractional change in the cohesive energy through  $T_\beta$ . If the labels  $\Delta N_g(T)$  and  $\Delta N_\beta(T)$  are used to denote the cumulative development of the new degrees of freedom at a temperature  $T$ , the combination of the two dilatational loss processes can be expressed to a first approximation as

$$B = B_e \left(1 - \frac{\Delta N_\beta(T)}{N_c}\right) \left(1 - \frac{\Delta N_g(T)}{N}\right) \quad (19)$$

Eq. (19) says simply that bulk modulus at low rates decreases relative to the ideal elastic form, due to energy dissipation as the degrees of freedom in the polymer change, and can be scaled in terms of temperature and rate by the distribution of the loss tangent through the transitions in Eq. (19), for example.

A similar logic is applied to calculate Young's modulus,  $Y$ . Again we start with the reference elastic parameter of  $B_e$  and calculate

the effect of mechanical energy dissipation through the transitions during uniaxial deformation, which serves to reduce the value of  $Y$  relative to  $B_e$ . A new GIM expression for Young's modulus below the glass transition,  $Y_\beta$ , has recently been published (Vollrath and Porter, 2005), which shows a direct relationship between  $Y$  and the combination of the elastic bulk modulus,  $B_e$  and the cumulative loss tangent through the beta transition,  $\int_0^T \tan \delta_\beta dT$ .

$$Y_\beta = B_e \cdot \exp\left(-\frac{\int_0^T \tan \delta_\beta dT}{A \cdot B_e}\right) \quad \text{where} \quad A = \frac{1.5 \times 10^5 L}{\theta_1 \cdot M} \quad (20)$$

Eq. (20) is derived from the proportionality between the temperature gradient of modulus and loss tangent, where  $A$  is the proportionality constant in terms of structural parameters that generally has values in the range  $1\text{--}2 \text{ GPa}^{-1}$  for most polymers, as in Eq. (11). Unfortunately, this simple proportionality breaks down as the Young's modulus reduces dramatically through  $T_g$ , such that a separate relation needs to be invoked for  $Y$  to cover temperatures through and above  $T_g$ . This relation is taken from the original GIM model that predicts the rubberlike plateau modulus above  $T_g$  due to the very high energy dissipation factor (loss tangent) through the glass transition, which has been shown previously to give good predictions of the rubberlike plateau modulus above  $T_g$  as a single continuous function through  $T_g$  (Porter, 1995)

$$Y = \frac{Y_\beta}{\left(1 + \int_0^T \tan \delta_g dT\right)^2} \quad (21)$$

The temperature and rate dependence of the engineering moduli are embraced by the rate dependence of the main transitions at  $T_\beta$  and  $T_g$ . At this stage all the applied strains are taken to be very small in the context of a dynamic mechanical analysis, DMA, such that the tensile and compressive values of  $Y$  are taken to be identical.

The bulk and tensile moduli are combined to give a predicted value of Poisson's ratio,  $\nu$ , using the standard relation

$$\nu = 0.5 \left(1 - \frac{Y}{3B}\right) \quad (22)$$

The combination of Poisson's ratio and  $B$  or  $Y$  can be used to predict any other modulus parameter if the polymer is taken to be an isotropic material. In addition, previous work has suggested that Poisson's ratio can be used to indicate the mode of failure under

tension;  $\nu < 0.38$  suggests a tendency to brittle failure (Porter, 1995).

Fig. 4 shows predictions of the dynamic properties of PC as solid lines for the tensile elastic modulus and loss tangent, noting that the loss tangent curves are plotted simply as the two relaxation peaks independently, without the low level thermomechanical contribution with a relatively constant value of the order 0.01 as a lower limiting baseline. The dashed lines in Fig. 4 are experimental data taken from Mulliken and Boyce for tensile modulus (Mulliken and Boyce, 2006) and a standard loss tangent curve (McRum et al., 1967). Predicted property values for PC at a typical temperature of  $T_0 = 300 \text{ K}$  and a strain rate of  $0.01 \text{ s}^{-1}$  are  $B = 3.9 \text{ GPa}$ ,  $Y = 2.1 \text{ GPa}$ , and  $\nu = 0.405$ .

Predicted tensile modulus values are often higher at low temperatures relative to dynamic mechanical spectra, but correspond well to modulus values obtained in tensile tests at normal ambient temperatures. We attribute this anomaly to excess free volume that is frozen into the polymer during sample preparation that cannot relax or 'age' at lower temperatures (Porter, 1995), and thereby maintains a too low value of modulus as temperatures are reduced relative to an ideally annealed sample for which predictions are relevant.

Fig. 5 illustrates the interrelations between the predicted values of dynamic mechanical properties ( $B_e$ ,  $B$ ,  $Y$ , and  $\nu$ ) for PMMA at a strain rate of  $0.01 \text{ s}^{-1}$ . Predicted property values at  $T_0 = 300 \text{ K}$  are  $B = 4.5 \text{ GPa}$ ,  $Y = 3.1 \text{ GPa}$ , and  $\nu = 0.376$ .

## 7. Constraints on loss history

Note that the model for engineering properties assumes that the polymer is in thermal equilibrium, and that the predicted properties are effectively those that are measured in a dynamic mechanical analysis, where sufficient thermal energy is available for the relaxation processes (changes in degrees of freedom) to develop fully at a specified temperature or rate/frequency. However, stress-strain tests are usually carried out at a constant temperature or high rate, where not all the degrees of freedom associated with the transitions may have developed. Thus, we need to show how these constraints affect the physical properties required to predict engineering stress-strain relations in polymers.

In a beta relaxation process, new skeletal degrees of freedom are activated through  $T_\beta$  in a first order temperature activated process given by Eq. (17). The glass transition process is different, in

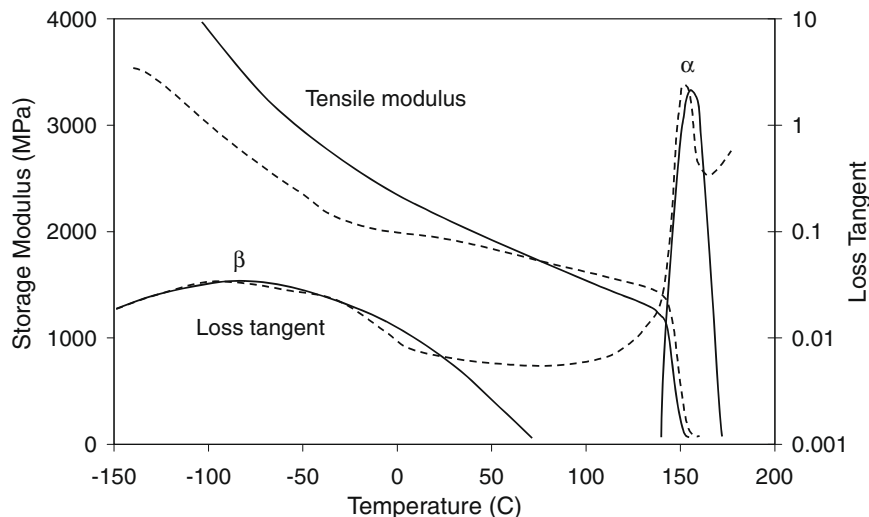


Fig. 4. Predicted values of dynamic mechanical properties for PC (solid lines), compared with experimental data (see text).

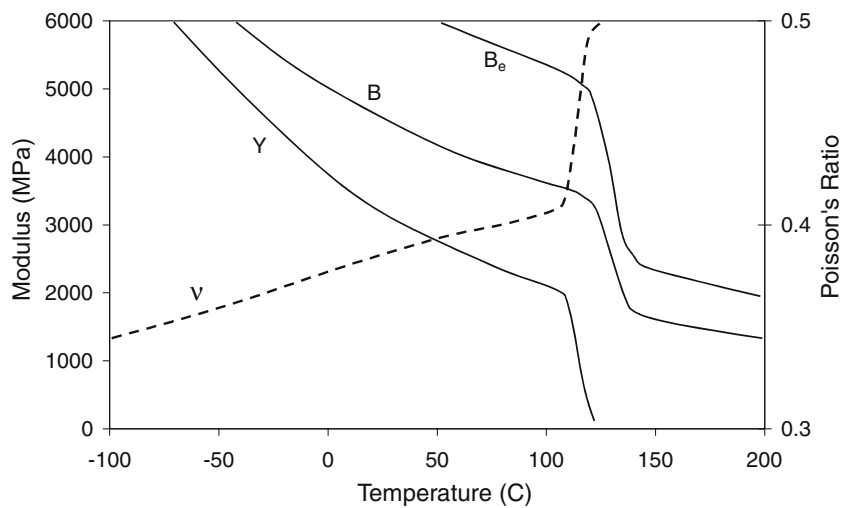


Fig. 5. Predicted values of dynamic mechanical properties for PMMA at a strain rate of  $0.01 \text{ s}^{-1}$ .

that new translational degrees of freedom are activated by a combination of thermal and mechanical energy corresponding to the elastic instability condition at a defined separation distance between groups of atoms. Since  $T_\beta$  increases at a rate of about  $15^\circ$  per decade of rate, relative to  $T_g$  increasing at a rate of only  $4^\circ$ , the  $T_\beta$  loss peak (and the associated increase in thermal energy due to new degrees of freedom) can often catch up with the  $T_g$  loss peak and the observation temperature,  $T_0$ . The effect of this coupling between  $T_\beta$  and  $T_g$  is that not all the extra degrees of freedom,  $\Delta N_\beta$ , may be activated at the temperature of measuring stress-strain relations,  $T_0$ , and is particularly important at higher rates of strain, which is equivalent to the Richeton et al. (2006) concept of cooperative relaxation. While this in no way affects the prediction of DMA spectra to validate the model, it has important effects upon the prediction of stress-strain relations.

The first consequence of limiting the beta relaxation degrees of freedom to their value at  $T_0$  is that the effective value of  $T_{gr}$  is shifted to a higher value by the lower effective value of  $N$  in Eq. (12). Similarly, tensile modulus is increased in Eq. (20) and thermal expansion is reduced in Eq. (5). We will see that these changes then also increase the yield stress and strain, and thereby can have a significant effect on the nonlinear rate dependence of mechanical properties. Therefore, it is important to note that the cut-off value of  $T_0$  must be used in any integration of beta degrees of freedom

and their consequent loss tangent parameters when predicting stress-strain relations at  $T_0$ . This is illustrated in Fig. 6, where the cumulative loss tangent predicted for PMMA reduces below the cut-off temperature  $T_0$  as rate increases.

Another important constraint on properties is that the extra degrees of freedom for the glass transition process are not activated if the observation temperature  $T_0$  is below  $T_g$ , such that properties such as thermal expansion coefficient do not increase significantly through yield, as seen in Fig. 1.

In order to specify the effect of thermal constraints on model parameters and properties, we use a subscript label  $\sigma$  for any property that has been calculated using constrained parameters in order to calculate the stress-strain response. The main constrained properties are  $\alpha_\sigma$ ,  $Y_\sigma$ , and  $\nu_\sigma$ .

### 8. Nonlinear stress-strain to yield

The predicted volumetric and dynamic mechanical properties now need to be transformed into large strain engineering stress-strain curves as a function of temperature and rate of strain. As a start, we will first predict stress-strain relations through the yield point without considering post-yield strain softening and hardening, which are discussed separately. To do this, strain and stress are predicted separately as a function of a dummy variable of a

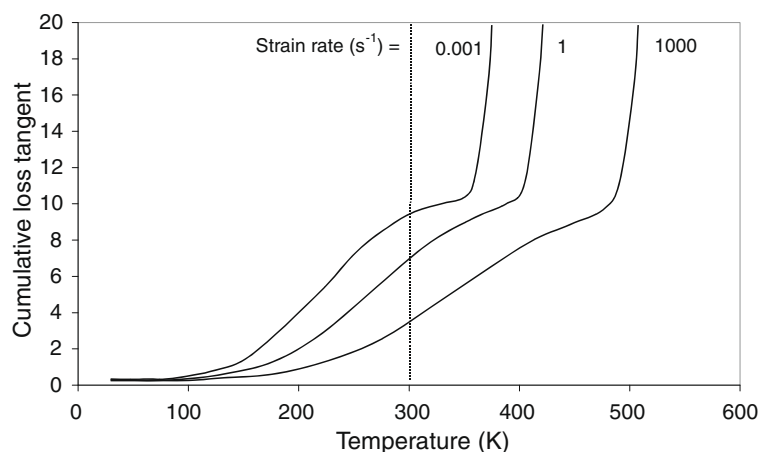


Fig. 6. Cumulative loss as a function of temperature at three different strain rates for PMMA, showing the reduction in effective value of loss with increasing rate at a typical operating temperature of 300 K (dotted lines).

temperature parameter in terms of the previously predicted physical properties of  $\alpha_\sigma$ ,  $Y_\sigma$ , and  $\nu_\sigma$ , which are thermal expansion coefficient, Young's modulus, and Poisson's ratio, respectively, but with their values constrained by the evolution of the degrees of freedom at a finite temperature  $T_0$  below  $T_g$ .

Strain,  $\varepsilon$ , is predicted using the potential function approach by taking strain to be equivalent to the thermal expansion over a temperature range. In this case, temperature is used as a dummy variable from the observation temperature,  $T_0$ , to an arbitrary maximum value well above  $T_g$ .

$$\varepsilon = \int_{T_0}^T \alpha_\sigma dT \quad (23)$$

Tensile stress,  $\sigma_t$ , is predicted using the Young's modulus over the strain equivalent to thermal expansion, again using temperature as a dummy variable, and that volumetric strain is used in combination with modulus that has been scaled relative to the bulk volumetric modulus

$$\sigma_t = \int_{T_0}^T Y_\sigma \alpha_\sigma dT \quad (24)$$

Transforming tensile stress to compressive stress has been tentatively linked to the pressure dependence of elastic modulus (Rich-

eton et al., 2006). However, the potential function approach of this work links the lower modulus at large tensile strains with the lower binding energy between interacting groups of atoms at increased separation distance. Thus, compressive stress,  $\sigma_c$ , is calculated from Eq. (24) using a factor  $2\nu_\sigma$  to adjust for expansion in the axes normal to the compression axis (Porter, 1995)

$$\sigma_c = \frac{\sigma_t}{2\nu_\sigma} \quad (25)$$

This deceptively simple formulation of strain and stress has proven to be very powerful as a predictive tool, and includes all the information about the polymer structure and the transition temperatures that dominate mechanical properties in engineering polymers.

### 9. Examples: PC and PMMA

To illustrate the quantitative capabilities of the model, two example polymers of PC and PMMA are presented below, and are chosen so that predictions can be compared directly with the work of Richeton et al. (2003, 2006, 2007) and Mulliken and Boyce (2006). Table 1 gives a list of the GIM parameter values for the two example thermoplastic polymers of PC, and atactic PMMA.

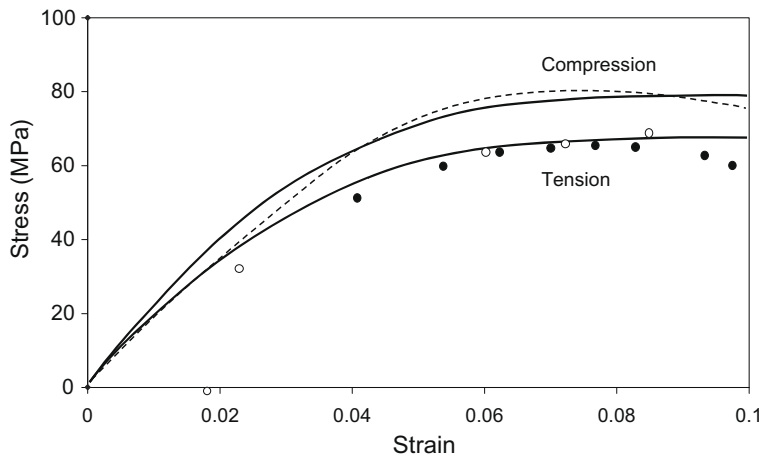


Fig. 7. Comparison of predicted stress–strain relations for PC at  $T_0 = 300$  K and a strain rate of  $0.01 \text{ s}^{-1}$  (solid lines) with experimental data in compression (dashed line; Richeton et al., 2006) and tension (points; Porter, 1995).

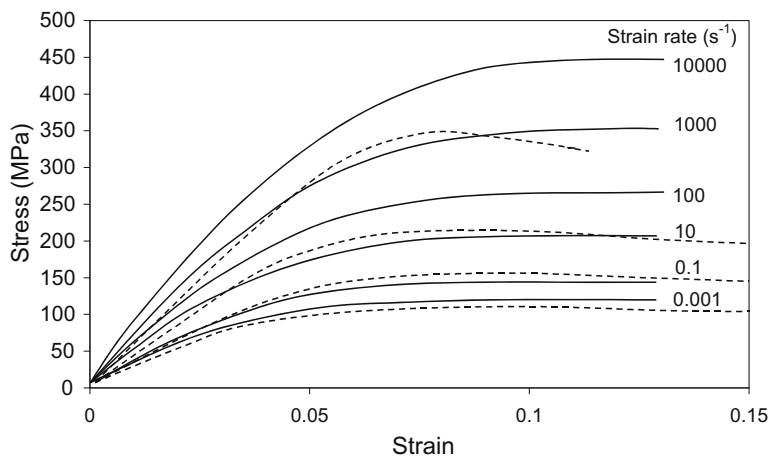


Fig. 8. Stress–strain predictions for PMMA at  $T_0 = 300$  K (solid lines) compared with experimental data of Richeton (dashed lines; Richeton et al., 2007) at a wide range of strain rates as labelled.

Fig. 7 plots the predicted tensile and compressive stress–strain relations for PC at 300 K and a strain rate of  $0.01 \text{ s}^{-1}$  without including the effect of strain softening or hardening. Experimental data under tension (Porter, 1995) and compression (Richeton et al., 2006) is also plotted in Fig. 7 under as near the same conditions as could be found in the literature.

Fig. 8 then plots the predictions for compressive stress–strain for PMMA for a wide range of strain rates from  $10^{-3}$  to  $10^4 \text{ s}^{-1}$  at a temperature of 300 K, which show a much higher plateau yield stress at high rates due to the synergy between the relaxation peaks as the beta relaxation catches up with the glass transition at high rates. Predicted solid lines show good agreement with published experimental data of Richeton et al. (2006), shown as dashed lines.

Figs. 9 and 10 then compare the predictions of yield stress for PC and PMMA as a function of rate at  $T_0 = 300 \text{ K}$  and as a function of temperature at a reference rate of  $0.01 \text{ s}^{-1}$ , and also shows experimental data from Richeton et al. (2006) and Mulliken and Boyce (2006) to demonstrate the overall capability of the model. Given the variability of the experimental data, the model predictions are reasonable. The main problem of predictions for PMMA is that atactic PMMA contains the two iso- and syndiotactic forms, which have very different values of  $T_g$  of 322 and 450 K, respectively, such

that relaxation effects between the two independent values is difficult to quantify without a more detailed set of relaxation functions for any specific PMMA sample.

### 10. Post-yield strain softening and hardening

At this stage in the model development, we introduce the general form of relations for post-yield behaviour of polymers that are consistent with the overall model framework. Above the glass transition and yield conditions, the molecular groups in the polymer attain new translational degrees of freedom in the chain axis and are able to translate relative to each other to allow macroscopic plastic flow, which causes stress relaxation above yield. The first problem here is to quantify the magnitude and rate of stress relaxation post-yield.

Figs. 7–9 show that yield stress increases with increasing rate due to the non-equilibrium conditions and their consequences upon the relaxation conditions. There is effectively a lower limiting yield stress at infinitely low strain rates that is the minimum stress at a specific temperature that can induce yield flow. Since the polymer group mobility increases rapidly and significantly above yield, we suggest that the yield stress at any finite strain rate must relax down to this lower limiting yield stress,  $\sigma_{y0}$ .

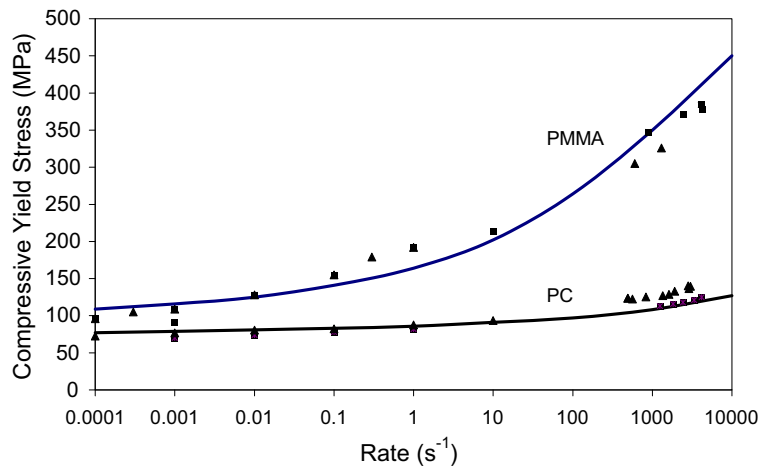


Fig. 9. Comparison of model predictions (lines) with experimental data (points) for the compressive yield stress of PC and PMMA as a function of strain rate at  $T_0 = 300 \text{ K}$ :  $\blacktriangle$ , data of Richeton et al. (2006);  $\blacksquare$ , data of Mulliken and Boyce (2006).

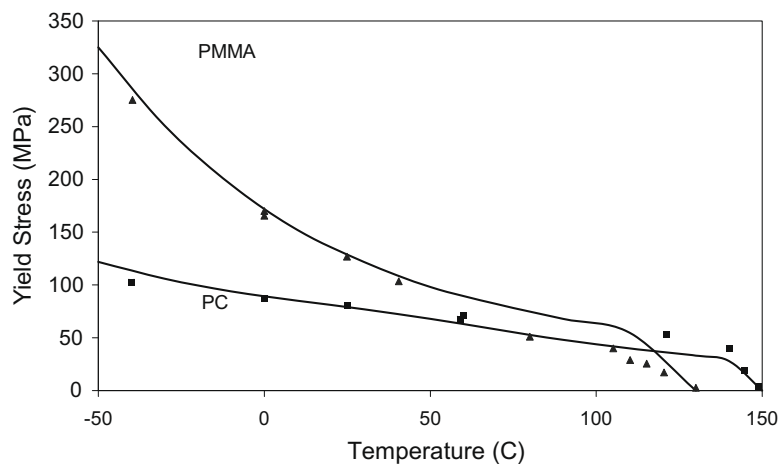


Fig. 10. Comparison of predicted (lines) and measured (points; Richeton et al., 2006) yield stress for PC and PMMA as a function of temperature at a strain rate of  $0.01 \text{ s}^{-1}$ .

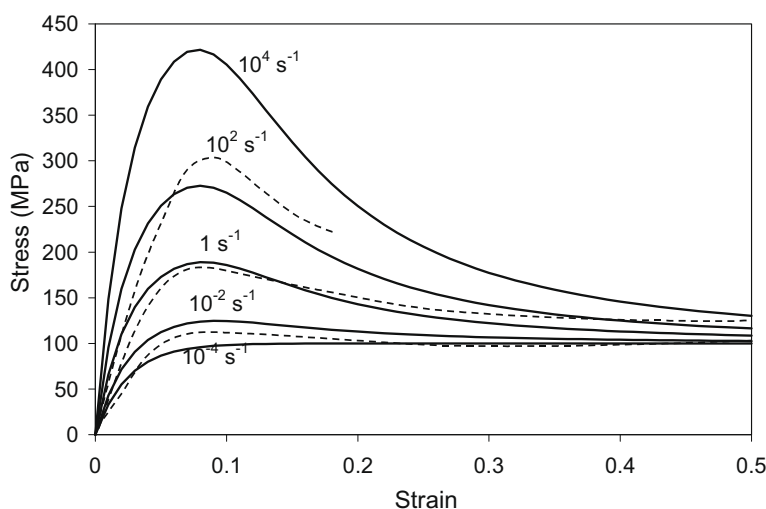


Fig. 11. Model predictions for the post-yield strain softening for PMMA at different strain rates at  $T_0 = 300$  K (solid lines) compared with experimental observations at approximately the same rates (Mulliken and Boyce, 2006).

The simplest way to estimate stress relaxation rate with strain is to assume that yield is an activated rate process with an activation energy,  $\Delta H_y$ , and that the probability of stress relaxation increases with increasing strain energy as more dynamic rubberlike states are generated. Since energy is proportional to strain squared, we suggest an expression for post-yield strain relaxation,  $\rho_y(\varepsilon)$  from  $\rho_{yr}$  at any rate  $r$  in terms of strain,  $\varepsilon$ , relative to an activation strain for yield,  $\varepsilon_{ya}$ , with a form

$$\sigma_y(\varepsilon) = \sigma_{y0} + (\sigma_{yr} - \sigma_{y0}) \exp\left(-\left(\frac{\varepsilon_{ya}}{\varepsilon}\right)^2\right) \quad (26)$$

A suitable value for  $\varepsilon_{ya}$  would be to predict the onset of strain softening at the strain where stress has reached its plateau value of yield stress at any rate of strain in plots like those shown in Figs. 7 and 8. The exponential decay form of Eq. (26) has the onset of stress relaxation at a value of about  $0.5\varepsilon_{ya}$ . This suggests a value of  $\varepsilon_{ya} \approx 0.14$  if the attainment of the yield stress is at a characteristic strain of around 0.07 in Figs. 7 and 8. Fig. 11 plots a model form of Eq. (26) for PMMA at a number of strain rates, using the yield stress of 100 MPa at a value of strain rate of 0.0001 for  $\sigma_{y0}$ , where Fig. 9 shows a trend to a limiting lower value for yield stress, which is in good general agreement with the experimental data and model forms presented by Mulliken and Boyce (2006) and Richeton et al. (2006).

Strain hardening in polymers can be attributed to reconversion of rubberlike states that are generated through the glass transition or yield process back into glassy or crystal states of matter as mechanical energy of deformation forces the groups of atoms back together under high strains (Porter, 1995; Vollrath and Porter, 2005). A general form for post-yield strain hardening was suggested in a recent refinement of the original GIM formulation for PC that was developed for spider silk polymers, which show very significant strain hardening to massive values of failure stress (Vollrath and Porter, 2005). However, the complex combination of stress relaxation due to dynamic post-yield rubberlike states and strain hardening due depletion of these states as a function of strain and strain rate is beyond the scope of this work, but the underlying mechanisms are consistent with the basis principles outlined in this paper.

## 11. Concluding remarks

The model presented here allows the highly nonlinear mechanical properties of polymers as a function of temperature, strain and

strain rate to be calculated directly from their molecular structure. The model is based upon the simple fundamental premise that mechanical properties are a direct consequence of energy stored and energy dissipated during deformation of a material. This premise is transformed into a consistent set of structure–property relations for the engineering constitutive relations in a polymer by quantifying energy storage and loss at the molecular level of interactions between characteristic groups of atoms in a polymer. By focussing the molecular level model directly on this premise, the constitutive relations can be formulated as a straightforward set of analytical equations that predict properties directly in terms of a very small set of structural parameters that can be calculated independently from the chemical composition and morphology of a polymer.

The combination of equation of state and nonlinear constitutive relations presented here can be applied directly to engineering simulation methods such as dynamic finite element simulations as a complete stiffness matrix for an isotropic polymer by using the combination of bulk and tensile moduli predicted here as a function of temperature, strain, and strain rate.

We have shown elsewhere that the basic model can be applied successfully to more complex polymers than the amorphous PC and PMMA examples presented here in a more developed form of the transformation of DTA to stress–strain properties. Semicrystalline polymers require additional relaxation temperatures to be included in the model to differentiate the crystal and amorphous transitions (Vollrath and Porter, 2005; Porter and Vollrath, 2008). Thermoset resins include the reduction of degrees of freedom due to branching or crosslinking sites (Jones, 2005; Foreman et al., 2006; Foreman et al., 2008). Validation examples for a wider range of such polymers using this model will be presented in future work, along with a broader discussion of post-yield strain softening and hardening. An energy density based failure initiation criteria has also been formulated for structural materials elsewhere in a form that is consistent with the model presented here (Porter, 1995, 2007). The combination of these different model elements will allow systematic design or optimisation of polymers for demanding structural engineering applications. In addition, the approach can be applied directly to complex biological materials, which offers considerable potential for biomechanics and bioengineering applications (Vollrath and Porter, 2005; Porter and Vollrath, 2008).

## Acknowledgments

Part of this work was carried out as part of the Weapons and Platform Effectors Domain of the MoD Research Programme. One of the authors (D.P.) would like to thank AFOSR for support on the work on silks, which is a key foundation for this work.

## References

- Arends, C.B., 1993. On the applicability of the Lennard-Jones potential function to amorphous high polymers. *Journal of Applied Polymer Science* 49, 1931–1938.
- Bauwens-Crowet, C., 1973. The compression yield behaviour of polymethyl methacrylate over a wide range of temperatures and strain-rates. *Journal of Materials Science* 8, 968–979.
- Bauwens-Crowet, C., Homes, G.A., 1964. La deformation plastique du polymethacrylate de methyle dans le domaine vitreux. *Academie des Sciences Comptes Rendus (Paris)* 259, 3434–3436.
- Bauwens-Crowet, C., Bauwens, J.C., Homes, G., 1969. Tensile yield stress behaviour of glassy polymers. *Journal of Polymer Science A 2* (7), 735–742.
- Bicerano, J., 1993. *Prediction of Polymer Properties*. Marcel Dekker, New York.
- Bicerano, J., Clark, H.A., 1992. Dynamic relaxations in poly(ester carbonates). In: Bicerano, J. (Ed.), *Computational Modelling of Polymers*. Marcel Dekker, New York, pp. 521–549.
- Bondi, A., 1968. *Physical Properties of Molecular Crystals, Liquids, and Glasses*. Wiley, New York.
- Born, M., 1939. Thermodynamics of crystals and melting. *Journal of Chemical Physics* 7, 591–601.
- Boyce, M.C., Parks, D.M., Argon, A.S., 1988. Large inelastic deformation of glassy polymers. *Mechanics of Materials* 7, 15–33.
- Carter, W.J., Marsh, S.P., 1997. Hugoniot Equation of State for Polymers. Los Alamos Report LA-13006-A.
- Eyring, H., 1936. Viscosity, plasticity, and diffusion as examples of absolute reaction rates. *Journal of Chemical Physics* 4, 283–291.
- Ferry, J.D., 1961. *Viscoelastic Properties of Polymers*. Wiley, New York.
- Foreman, J.P., Porter, D., Behzadi, S., Travis, K.P., Jones, F.R., 2006. Thermodynamic and mechanical properties of amine-cured epoxy resins using group interaction modelling. *Journal of Materials Science* 41 (20), 6631–6638.
- Foreman, J.P., Porter, D., Behzadi, S., Jones, F.R., 2008. A model for the prediction of structure–property relations in cross-linked polymers. *Polymer* 49, 5588–5595.
- Hutnik, M., Argon, A.S., Suter, U.W., 1991. Quasi-static modelling of chain dynamics in the amorphous glassy polycarbonate of 4,4'-isopropylidenediphenol. *Macromolecules* 24, 5970–5979.
- Jones, F.R., 2005. Molecular modelling of composite matrix properties. In: Soutis, C., Beaumont, P.W.R. (Eds.), *Multi-Scale Modelling of Composite Material Systems*. Woodhead Publishing Ltd., Cambridge, pp. 1–32.
- McRum, N.G., Read, B.E., Williams, G., 1967. *Anelastic and Dielectric Effects in Solid Polymers*. Wiley, London.
- Mulliken, A.D., Boyce, M.C., 2006. Mechanics of the rate-dependent elastic-plastic deformation of glassy polymers from low to high strain rates. *International Journal of Solids and Structures* 43, 1331–1356.
- Porter, D., 1995. *Group Interaction Modelling of Polymer Properties*. Marcel Dekker, New York.
- Porter, D., 2007. Multiscale modelling of structural materials. In: Guo, Z.X. (Ed.), *Multiscale Materials Modelling*. Woodhead Publishing Ltd., Cambridge.
- Porter, D., Gould, P.J., 2003. Multiscale modelling for equations of state. *Journal de Physique IV France* 110, 809–814.
- Porter, D., Gould, P.J., 2006. A general equation of state for polymeric materials. *Journal de Physique IV France* 134, 373–378.
- Porter, D., Vollrath, F., 2008. The role of kinetics of water and amide bonding in protein stability. *Soft Matter* 4, 328–336.
- Ree, T., Eyring, H., 1955. Theory for non-Newtonian flow: I. Solid plastic system. *Journal of Applied Physics* 26, 780–793.
- Richeton, J., Ahzi, A., Daridon, L., Remond, Y., 2003. Modelling of strain rates and temperature effects on the yield behaviour of amorphous polymers. *Journal de Physique IV France* 110, 39–44.
- Richeton, J., Ahzi, S., Daridon, L., Remond, Y., 2005. A formulation of the cooperative model for the yield stress of amorphous polymers for a wide range of strain rates and temperatures. *Polymer* 46, 6035–6043.
- Richeton, J., Ahzi, A., Vecchio, K.S., Jiang, F.C., Adharapurapu, R.R., 2006. Influence of temperature and strain rate on the mechanical behaviour of three amorphous polymers. *International Journal of Solids and Structures* 43, 2318–2335.
- Richeton, J., Ahzi, A., Daridon, L., 2007. Thermodynamic investigation of yield stress models for amorphous polymers. *Philosophical Magazine* 87, 3629–3643.
- Roetling, J.A., 1965a. Yield stress behaviour of polymethyl methacrylate. *Polymer* 6, 311–317.
- Roetling, J.A., 1965b. Yield stress behaviour of polyethyl methacrylate in the glass transition region. *Polymer* 6, 616–619.
- Roetling, J.A., 1966. Yield stress behaviour of isotactic polypropylene. *Polymer* 67, 303–306.
- Seitz, J.T., 1993. The estimation of mechanical properties of polymers from molecular structure. *Journal of Applied Polymer Science* 49, 1331–1351.
- Soong, S.Y., Cohen, R.E., Boyce, M.C., Mulliken, A.D., 2006. Rate-dependent deformation behaviour of POSS-filled and plasticized poly(vinyl chloride). *Macromolecules* 39, 2900–2908.
- Theodorou, D.N., Suter, U.W., 1985. Detailed molecular structure of a vinyl polymer glass. *Macromolecules* 18, 1467–1478.
- Theodorou, D.N., Suter, U.W., 1986. Atomistic modelling of mechanical properties of polymeric glasses. *Macromolecules* 19, 139–154.
- van Krevelen, D.W., 1993. *Properties of Polymers*, third ed. Elsevier, Amsterdam.
- Vollrath, F., Porter, D., 2005. Spider silk as a model biomaterial. *Applied Physics A* 82, 205–212.
- Walley, S.M., Field, J.E., 1994. Strain rate sensitivity of polymers in compression from low to high rates. *DYMAT Journal* 1, 211–227.
- Walley, S.M., Field, J.E., Pope, P.H., Safford, N.A., 1989. A study of the rapid deformation behaviour of a range of polymers. *Philosophical Transactions of the Royal Society London A* 328, 1–33.
- Walley, S.M., Field, J.E., Pope, P.H., Safford, N.A., 1991. The rapid deformation behaviour of various polymers. *Journal de Physique III France* 1, 1889–1925.
- Wu, S., 1990. Chain structure, phase morphology, and toughness relationships in polymers and blends. *Polymer Engineering and Science* 30, 753–761.
- Wu, S., 1992. Secondary relaxation, brittle–ductile transition temperature, and chain structure. *Journal of Applied Polymer Science* 46, 619–624.
- Wunderlich, B., Cheng, S.Z.D., Loufakis, K., 1989. *Encyclopaedia of Polymer Science and Engineering*. Wiley–Interscience, New York.
- Zerilli, F.J., Armstrong, R.W., 2007. A constitutive equation for the dynamic deformation behaviour of polymers. *Journal of Materials Science* 42, 4562–4574.